Journal of Intelligent Systems and Control
https://www.acadlore.com/journals/JISC

Dynamic Modelling of Permanent Magnet Synchronous Motors with Graphical Simulation Validation

S. Jasphin Melba[1*], A. Ravi [2], Shibu J.V. Bright [1]

[1] Electrical and Electronics Engineering, Maria College of Engineering and Technology, 629177 Attoor, India
[2] Electrical and Electronics Engineering, Francis Xavier Engineering College, 627003 Vannarpettai, India

[*] Correspondence: S. Jasphin Melba (sjm.research2023 @gmail.com)

Received: 02-03-2025 **Revised:** 03-07-2025 **Accepted:** 03-15-2025

Citation: S. J. Melba, A. Ravi, S. J. V. Bright, "Dynamic modelling of permanent magnet synchronous motors with graphical simulation validation," *J. Intell Syst. Control*, vol. 4, no. 1, pp. 21–33, 2025. https://doi.org/10.56578/jisc040103.

Abstract: Permanent Magnet Synchronous Motors (PMSMs) have garnered sustained attention over the past four decades due to their high efficiency, superior torque density, and dependable operational characteristics, making them highly suitable for a wide range of industrial applications. Accurate dynamic modelling of PMSMs is essential for performance evaluation and the development of advanced drive control strategies. Although previous studies have addressed customized modelling approaches for various PMSM types, a streamlined method for deriving model parameters from standard manufacturer specifications remains insufficiently explored. As a result, simulation studies are often disconnected from commercially available motor data, thereby limiting their practical relevance. In this study, the dynamic model of a PMSM is reformulated within the synchronous rotating reference frame (d-q axis) and implemented using mathematical function blocks in the MATLAB/Simulink environment. A systematic procedure is developed to extract key motor parameters from typical manufacturer data sheets. This approach bridges the gap between theoretical modeling and real-world motor implementation. The proposed modelling framework is validated using a standard 1 hp, 2.2 Nm, 1500 rpm PMSM, and its performance is benchmarked against the built-in Simulink PMSM blockset. Simulations are conducted to evaluate the mechanical output, rotor speed, and electromagnetic torque responses under step variations in load torque. The results exhibited strong agreement between the custom mathematical model and the blockset counterpart, confirming the accuracy and practical applicability of the parameter extraction methodology.

Keywords: Permanent magnet synchronous motor; Dynamic modelling; d-q reference frame; Parameter extraction from specifications; MATLAB/Simulink simulation; Model validation; Torque-speed characteristics; Custom vs. blockset model comparison

1 Introduction

Due to the high-paced industrial automation, the electrical drive systems have been widely studied and contemplated [1]. The application ambit of drives has straddled widely in several fields such as robotics [2], electrical vehicles [3], automation equipment [4], material handling [5], air conditioning and refrigeration [6], rolling mills [7], wind energy conversion systems [8], aerospace [9], domestic appliances [10], etc. The technical feasibility of manufacturing permanent magnetic materials with the required strength and shape, combined with digital controllers, has made PMSMs a potential alternative to the induction motor in many applications [11]. PMSMs are preferred due to their merits such as improved power density (compactness), increased torque-to-inertia ratio, high efficiency (minimal losses and heat dissipation), easy maintenance, and reliability [12]. Aforementioned details urge both the establishment of the PMSM simulation model and the subsequent development of application driven control systems, hence satisfying/customising the system requirements [13].

A mathematical (equation) model of an electric motor is basically a set of equations that represents the dynamics of the system accurately, including the coupled, nonlinear, intertwined relationships amid voltages, currents, and motor inductances. From these basic equations of the pristine motor, the model for the nascent motors with structural modifications can be deduced appropriately. The other characteristics for those improved versions can always be obtained from the original characteristics even for their nuance in the design structure and/or the material selection [14, 15]. Different modelling approaches are available, namely, the d-q synchronous rotating frame model, the stationary two-axis model [16], the arbitrary reference frame model, the finite element analysis (FEA) patronal neutral network model [17], etc. Researchers in the field of Alternating Current (AC) motor dynamic have vehemently asserted the conduciveness of the synchronous rotating frame model for both research and control problems of motors. The complex time-varying nature of AC motor dynamics becomes much simpler to analyse and control when represented in the rotating d-q frame. Hence the basic dynamic model for any poly phase machine, including the PMSM, is actualised in a two-phase machine analogy, which is well accepted because it enables a straightforward understanding of the working with the two-winding arrangement. The merit of this model is the precise alignment of the magnetic field produced by the stator currents with the desired rotor flux, which enables the prediction of the optimal torque requirement at any loading condition. This leads to the extraction of two-axis currents as Direct Current (DC) quantities.

Amid two categories of permanent magnet motors, i.e., the PMSM and the brushless DC motor (BLDCM), the PMSM does have the sinusoidal back electromotive force (BEMF) while the BLDCM has the trapezoidal BEMF [18]. Additionally, the BLDCM requires a rectangular stator current to produce the smooth electromagnetic torque. Due to the inherent self-controlled operation in the field-oriented control (FOC), the damper winding in the PMSM is not considered gratuitously. Therefore, the basic d-q PMSM model can be obtained from the pristine synchronous machine equations by removing the terms pertaining to the damper winding and the field current. Simple equivalent circuits for two categories of PMSMs, namely, PMSMs with the projecting magnet (surface mount) rotor and the imbedded magnets rotor, along with high-energy rare-earth magnets, have been developed along with experimental verification [19].

Bowen et al. [20] illustrated the model and the simulation study of the PMSM based on the state space technique. Both Park and Clark transformations were employed in deciding the initial conditions wherein their motive was modelling and simulating the space-space controlled six-step inverter fed PMSM drive. Zhang et al. [21] actualised the state-space model and a speed controller for the FOC-inverter drive fed PMSM. Performance differences amid twosome inverter drive mode, i.e., pulse width modulation (PWM)-based operation and hysteresis current controller-based operation, were examined. Even a subtle deviation in the PMSM parameters due to the inaccurate estimation, d- and q-axis inductances, phase angle of stator current and stator winding resistances, can influence electromagnetic torque and rotor speed [22]. Hence, it is commonly recommended to involve FEA for the parameter computation in the dynamic modelling. The model suggested by Dutta and Tripathi [23] has accounted the core saturation and successfully demonstrated the effect of the included core loss resistance in the PMSM performance. The influence of PMSM parameters, namely, stator resistance, flux linkage, d axis inductances and q axis inductances, on the control was recognised during their changes caused by skin effect, magnetic saturation, temperature variations, etc [24]. The necessity of accurate parameter computation was highlighted by involving a Chaotic Gaussian-Cauchy RAO algorithm in the parameter identification process of PMSMs. Deep learning neutral network has improved the parameter estimation of PMSMs more accurately than earlier attempts [25].

However, the motor parameters are easily affected by temperature changes, skin effect, and magnetic saturation, which can lead to poor control performance of the Proportional-Integral-Derivative (PID) controller and thus affect the motor's operating performance. Therefore, to achieve high dynamic response and high-precision control, accurate motor parameters are needed, and fast and effective parameter identification methods are required to improve the control performance of the entire servo system.

Apart from selecting the pertinent model for the study, deeper knowledge on the model and savvy to customise same is mandatory for researchers due to the reasons below. Researchers need to develop the control structure for the drive system, monitor the system, suggest protective arrangements, and determine the rating of different modules in the application under study. In this study, the synchronous rotating frame-based dynamic model is rekindled for the surface-mounted PMSM. The lucid model developed was schematised in the MATLAB-Simulink platform and customised for obtaining the basic system variables (line voltages/currents, torque, speed, etc.). A formulaic procedure was also suggested in this study for obtaining parameters required for the simulation study from the typical specification tables of the commercial PMSMs. The extracted motor parameters were fed to the schematised model as wells as the built-in PMSM blockset model of the Simulink. As the ultimate focus of this study is to assertion an accurate study platform for the PMSM research, these two motor replications, i.e., the equation-based mathematical replication and the built-in blockset of the Simulink, were critically compared in this study.

2 PMSM

Like any three-phase motor such as the induction motor and the wound rotor synchronous motor (WRSM), the stator of the PMSM does accommodate the three-phase distributed winding. The rotor of the PMSM does have permanent magnets made of rare-earth materials with very high resistivity, which makes the induction in the rotor negligible. The BEMF established by the permanent magnet and the one established by the distributed windings can be considered as the same. This enables that the treatment of the mathematical models of the PMSM and the

WRSM is similar. In the PMSM rotor, the magnetic flux is ascertained by permanent magnets, which makes the PMSMs brushless. This brushless excitation not only makes the rotor free from winding arrangements but also helps in increasing the power density, which in turn reduces the size and weight. The absence of rotor copper losses patronages in efficiency enhancement. Amid the variety of PMSM rotor options, the surface-mounted PMSM bestows the merit, i.e., low construction cost compared to its counterpart—the inset type. Due to the chance of detaching the rotor permanent magnets particularly at high rotor speeds, surface-mounted type rotors are not recommended for high-speed applications. The mounting is supported by the saliency created in the core structure, which helps in managing the stress caused by the centrifugal forces. Hence, the associated design can support little higher speed ranges.

3 Mathematical Modelling of the PMSM

A thorough knowledge of the motor design and working and the dynamic model are prerogatives for the engineers practicing in the electric drive field. To have a simplified analysis, the PMSM was modelled in the synchronous reference (d-q) frame of the rotor, which transforms all the variables into DC quantities simultaneously. The PMSM model commonly consists of three sets of equations, namely, the voltage equation set, the flux linkage equation set, and the motion equations. If the PMSM model is derived from the most familiar induction motor model, it will be conducive for the readers. As both constructional and behavioural features of the PMSM stator is identical to that of an induction motor, the d-q axis model of the PMSM stator is the same as that of the induction motor. Figure 1 and Figure 2 show the q and q-axis equivalent circuits of the induction motor.

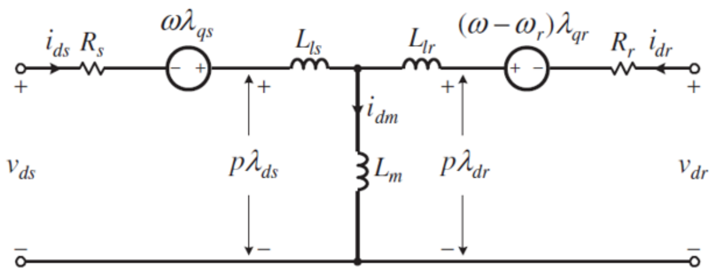

Figure 1. Per phase d-axis equivalent circuit of the induction motor

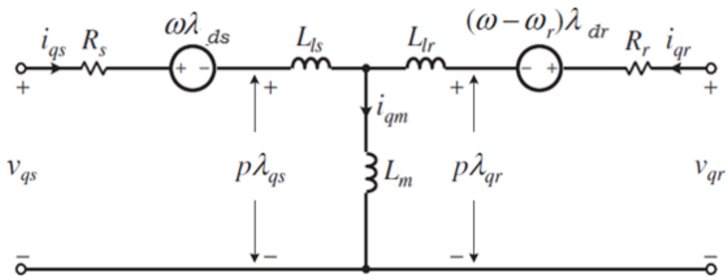

Figure 2. Per phase q-axis equivalent circuit of the induction motor

Figure 3 represents the d-q frame model of the synchronous motor. In the induction motor model, the speed (ω) of the arbitrary reference frame can be replaced by the rotor speed (ω_r) to obtain the model in the rotor synchronous frame. The magnetising inductance of the induction motor, L_m (in H), was replaced with the d- and q-axis magnetising inductances, L_{dm}(in H) and L_{qm} (in H) of the PMSM. It is worth to note that in case of cylindrical synchronous motors, the d-and q-axis magnetising inductances are equal $(L_{dm} = L_{qm})$, while in the case of salient-pole motors, the d-axis magnetising inductance is normally lesser than the q-axis magnetising inductance $(L_{dm} < L_{qm})$. L_{ls} and L_{lr} are the leakage inductances of the stator and rotor windings, respectively, in H; I_{dm} and I_{qm} are currents (in A) in L_{dm} and L_{qm}, respectively; R_s and R_r are the stator and rotor resistances, respectively, in Ω; and I_{ds} (I_{qs}) and I_{dr} (I_{qs}) are the stator and rotor d (q) axis components of currents, respectively, in A. In the PMSM, the permanent magnets were used to replace the field winding in the WRSM, which can be modelled by an equivalent current source with a fixed current magnitude, If (in A), to have the identical flux linkage, f (in wb), of the WRSM.

The equations for the stator voltages were arrived in terms of the d-axis (V_{ds}) and q-axis (V_{qs}) components.

$$V_{ds} = R_s i_{ds} - \omega_r \lambda_{qs} + \rho\lambda_{ds} \tag{1}$$

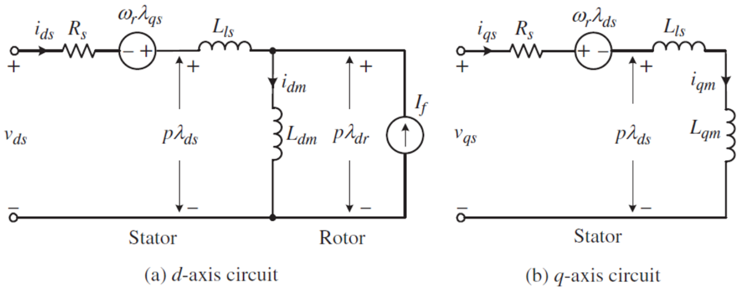

Figure 3. Rotor synchronous reference frame (d-q axis) model of the synchronous motor

$$V_{qs} = R_s i_{qs} + \omega_r \lambda_{ds} + \rho \lambda_{qs} \tag{2}$$

where, λ_{ds} and λ_{qs} are the d- and q-axis stator flux linkages (in wb), respectively. The flux linkages of the d- and q-axis stator windings can be computed by adding the flux linkages due to their respective excitation and mutual flux linkages caused from other winding's current and excitation current equivalent to permanent magnets.

$$\lambda_{ds} = L_{ls} i_{ds} + L_{dm} \left(i_f + i_{ds}\right) = L_d i_{ds} + \lambda_r \tag{3}$$

$$\lambda_{qs} = \left(L_{ls} + L_{qm}\right) i_{qs} = L_q i_{qs} \tag{4}$$

where, λ_{ris} indicates the flux linkage in rotor (in wb); and L_{dd} and L_{aa} are the d- and q-axis self-inductances (in H), respectively. Relations between the above-mentioned flux linkage and self-inductances are as follows:

$$\lambda_r = L_{dm} i_f \tag{5}$$

$$L_d = L_{ls} + L_{dm} \tag{6}$$

$$L_q = L_{ls} + L_{qm} \tag{7}$$

With the substitution of Eqs. (3) and (4) in Eqs. (1) and (2) and also considering $d\lambda r/dt = 0$ at fixed If and λr values, V_{ds} and V_{qs} can be obtained.

$$V_{ds} = R_s i_{ds} - \omega_r L_q i_{qs} + \rho L_d i_{ds} \tag{8}$$

$$V_{qs} = R_s i_{qs} + \omega_r L_d i_{ds} + \omega_r \lambda_d + \rho L_q i_{qs} \tag{9}$$

Figure 4 portrays an uncomplicated model for the synchronous motor, which can be obtained from Eqs. (8) and (9). The circuits shown in Figure 4 are straightforward representations of the general d- and q-axis model equations pertaining to the rotor synchronous reference frame.

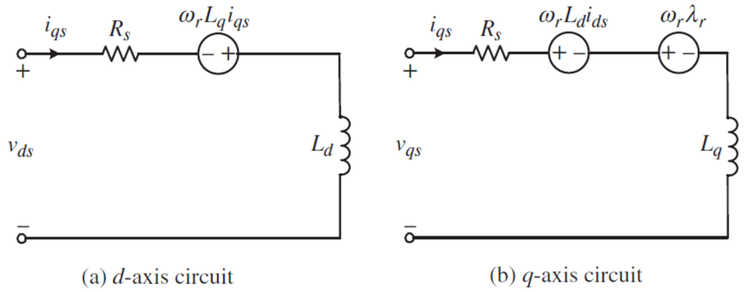

Figure 4. A bridged d-q axis model of the synchronous motor

The electromagnetic torque (T_e) is the imperative output variable, which governs the dynamics of the motor in terms of the rotor position speed.

$$T_e = \frac{3}{2}\frac{P}{2}\left[\lambda_{ds} i_{qs} - \lambda_{qs} i_{ds}\right] \tag{10}$$

where, P is the number of poles. Substitution of the flux linkages in terms of the inductances and current yields the following electromagnetic torque equation in N-m.

$$T_e = \frac{3}{2}\frac{P}{2}\left[\lambda_{af} i_{qs} + (L_{dm} - L_{qm})\, i_{qs} i_{ds}\right] \tag{11}$$

where, two terms constitute the electromagnetic torque, namely, the permanent magnet torque component and the reluctance torque component. The first term is constituted by the product of the q-axis current and the flux linkage. The second term is influenced by the product of the difference between the d- and q-axis inductances and currents.

The basic torque balance equation is presented in Eq. (12).

$$T_e = T_L + J\frac{d\omega_m}{dt} + B\omega_m \tag{12}$$

where, T_L is the load torque (in Nm); J is the moment of inertia (in $\mathrm{kg \cdot m^2}$); B is the viscous friction coefficient $(\mathrm{Nm - s/rad})$; and m is the measured speed of the motor. The rotor mechanical speed is given by Eq. (13).

$$\omega_m = \int \left(\frac{T_e - T_L - B\omega_m}{J}\right) \tag{13}$$

Figure 5 shows the basic block diagram of the PMSM model which have four sub-blocks. These sub-blocks represent the axis transformation, the flux calculation in d-q axes corresponding to d- and q -axis currents and the computation of mechanical variables. The additional feed back block is used to determine the position from the (rotor) speed information. For the input load torque (T_L) and the three-phase supply voltage $(V_a, V_b$, and $V_c)$, the model provides the electromagnetic torque and rotor speed as outputs.

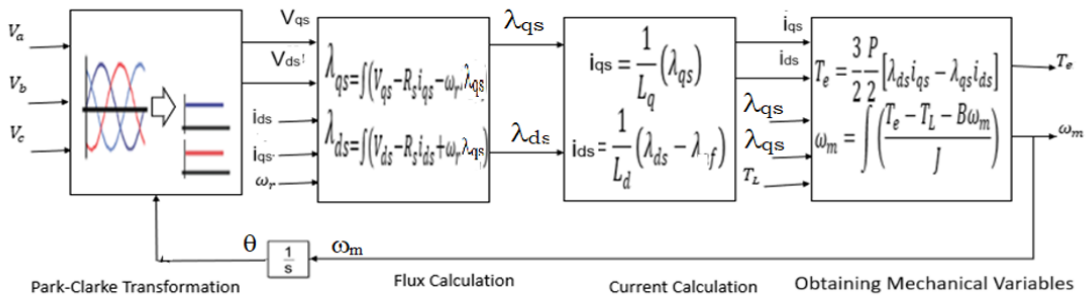

Figure 5. PMSM modelling as the block diagram

4 Obtaining Motor Parameters from the Datasheet

Any motor is a heterogeneous dynamic system, which includes the interaction of electromagnetic and mechanical variables. Typical model equations involve electrical, magnetic, and mechanical parameters of the PMSM. The various electrical parameters and constants are $R_s(\Omega)$, stator inductance $L_s(\mathrm{H})$, BEMF constant $K_b(\mathrm{~V-s/rad})$, electrical time constant $\tau\_a(\mathrm{~s})$, etc. The mechanical parameters and constants are J, B, torque constant $KT(\mathrm{Nm/A})$, mechanical time constant $\tau\_m(\mathrm{~s})$, etc. The data of the manufacturer specifications are sometimes insufficient or indirect for incorporating the model in the entirety. The unavailability of the required procedure for obtaining model parameters hindered the study as the direct measurement of few parameters are cumbersome at operating conditions. However, the lingering data can be computed inventively. A formulaic procedure was coined to obtain the required information which is not directly given on the motor nameplate. R_s accounts the per phase resistance obtained between a line and the neutral. It is a common practice that in PMSMs, the neutral of star-connected stator winding is not taken out for the access and thus the resistance has to be measured between line-to-line.

$$R_s = \frac{1}{2}R_{LL} \tag{14}$$

The synchronous axis inductances, L_d and L_q, can be obtained from the line-to-line inductance, as two-thirds of L_{LL}, respectively, at the rotor angle θ (electrical) values 0 degree and 90 degrees.

$$L_d = \frac{2}{3}L_{LL} \text{ at } \theta = 0^\circ \tag{15}$$

$$L_q = \frac{2}{3} L_{LL} \text{ at } \theta = 90^\circ \tag{16}$$

The synchronous inductances of the surface-mounted PMSM are almost equal because the permanent magnets are surface mounted and the reluctance is the same in every position. The BEMF constant, Kb (V-s/rad), was computed by measuring the no-load line voltage induced across the motor's line terminals while the motor is rotated through its shaft at a constant speed of ωm. For determining the mechanical parameters, J and B, several online and offline methods were suggested by researchers [26]. The constant represents the ratio between BEMF and the angular electrical frequency/speed. Table 1 shows the specification of the PMSM used in this study. This kind of 1 hp motors are very attractive in Indian subcontinent and its Ministry of New and Renewable Energy (MNRE) has approved it for solar submergible pumps. The cross-sectional view of a typical PMSM is shown in Figure 6.

Table 1. Specifications of the subsumed PMSM

Parameter	Symbol (Unit)	Value
Power rating	Pr (hp)	1
Stator voltage rating	Vs (V)	220
Stator current rating	Is (A)	3.69
Speed rating	Nr (rpm)	1500 @ 50 Hz
Torque rating	Tr (Nm)	2.2
Stator resistance	RLL (Ω)	5.55
q-axis inductance	LLL at $900(\mathrm{mH})$	3.285
d-axis inductance	LLL at $00(\mathrm{mH})$	3.285
Number of poles	P	4
Permanent magnet flux	f (wb)	0.140
BEMFconstant	$\mathrm{Kb(V - s/rad)}$	36
Torque constant	Kt (Nm/A)	0.60
Electrical time constant	e (s)	2.14 ms
Mechanical time constant	m (s)	1.8 ms
Motor of inertia	J $\mathrm{kg - m^2})$	0.028
Viscous damping coefficient	B (N-s/m)	0.000334

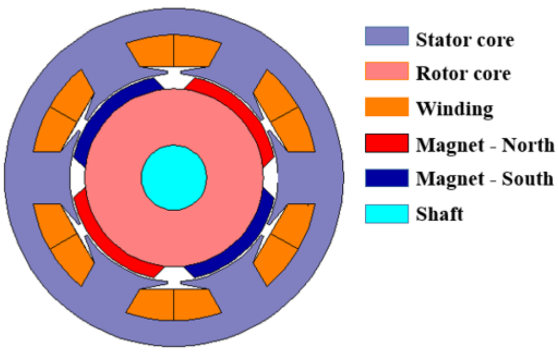

Figure 6. Cross-sectional view of the PMSM

5 Simulation Study and Corroboration of the Developed Model

After performing the comprehensive rekindling of the model and determining appropriate parameters, a systematic schematisation can lead to the verification of the model by comparing the results with the performance of the PMSM Simulink library blockset model after feeding the system parameters. The suggested PMSM model was schematised in the graphical programming platform, Simulink (MATLAB 2018a), using the ordinary differential equation (ODE) solver ode23tb with a start time of 0 s and a stop time of 0.3 s in the variable-step simulation. The mathematical equations were transferred into the Simulink schematic using the appropriate blocks available in the library and the comprehensive design is demonstrated in Figure 7.

The result corresponding to rated output condition is illustrated as a representative case in this section. Figure 8 to Figure 10 demonstrate the results of the model, wherein Figure 8 shows the three-phase supply voltages and their corresponding d-q frame components after the Park-Clarke transformation. The red coloured waveforms belong to the q-axis while the blue coloured ones are the d-axis components. Figure 9 pictures d- and q-axis currents and flux linkage components. Figure 10 presents the response in terms of both electromagnetic torque and speed at the rated operating condition. The results confirm the values of Tr(2.2 Nm) and Nr(1500 rpm).

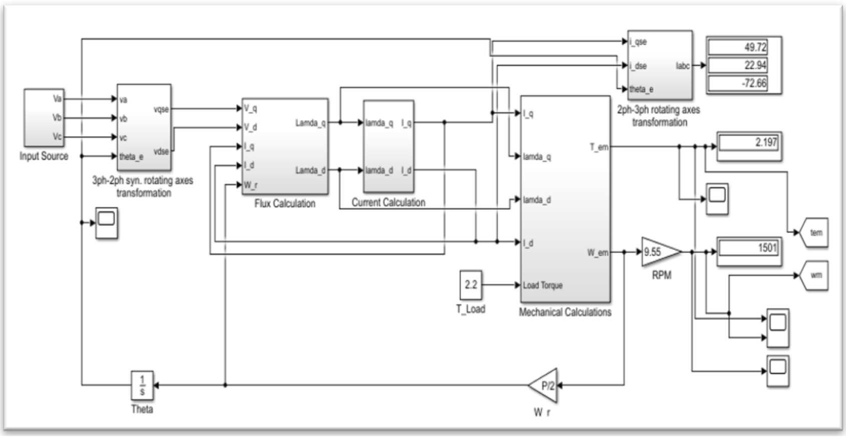

Figure 7. Schematisation of the PMSM model in the Simulink editor

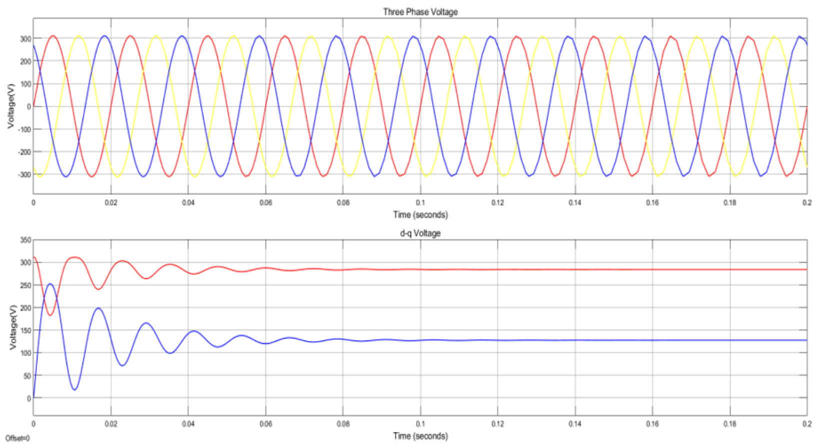

Figure 8. Input and output of the Park and Clarke transformation sub-block

To facilitate an effective comparison, a dual-model schematic comprising an equation-based model and a Simulink blockset model was developed and is presented in Figure 11. This comparison bestows several interesting results for the ready reference. Figure 12 to Figure 14 show the comparison amid results obtained from the mathematical model and the Simulink blockset model. The red waveform corresponds to the mathematical model while the blue waveform corresponds to the blockset model. The responses of the mathematical model closely match with the blockset model. Table 2 explores the effectiveness of the developed mathematical model by comparing its error (%) and convergence time with the Simulink blockset model. Figure 15 shows the torque and speed responses for the change in the torque reference from 2.2 Nm to 4 Nm at 1 second. In the open loop operation of the model after the transition, both torque and speed settle. Figure 16 and Figure 17 show the representative stator phase currents and their harmonic spectrum, respectively, obtained from the equation model and the blockset model schematics. Both cases have the same total harmonic distortion (THD) as 1.73%. The lowest line current harmonics $\left(5^{\text{th}} \text{ and } 7^{\text{th}}\right)$ are negligibly minimum, which are 0.55% and 0.28%, respectively. The startup transient behaviours of torque and speed are depicted in Figure 18 and Figure 19, respectively, for the equation model and the blockset model. Figure 18 and Figure 19 show the Time Domain Specifications (TDSs).

6 Conclusion

The structural configuration of the PMSM closely resembles that of a conventional wound rotor synchronous machine, with the key distinction being the use of embedded permanent magnets for field excitation in place of windings, and the absence of damper windings. The d-q model of the PMSM was obtained from the d-q axis model of the synchronous machine just by removing the terms pertaining to the damper windings and field current

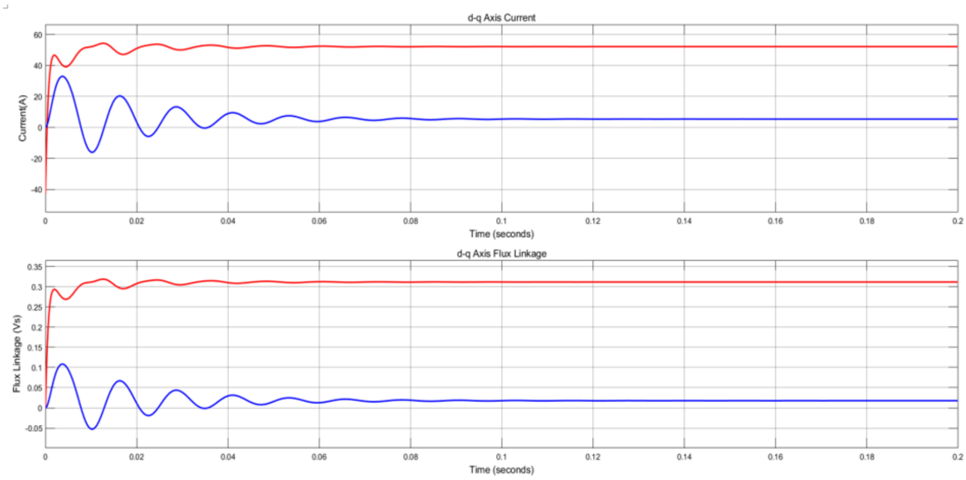

Figure 9. d- and q-axis currents and flux linkages

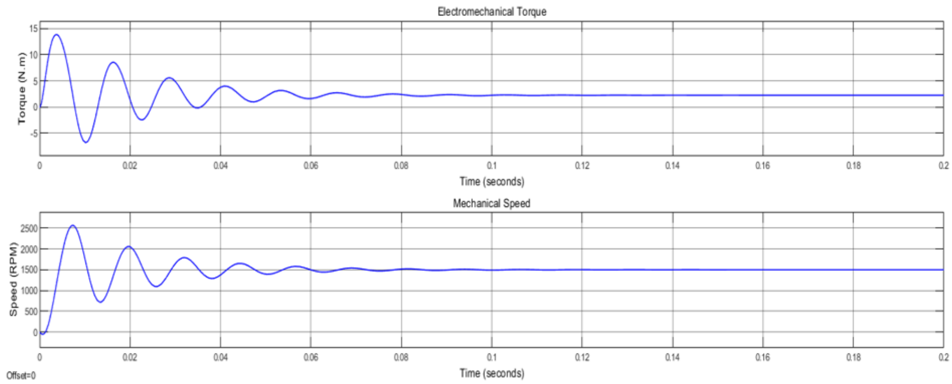

Figure 10. Electromagnetic torque and speed

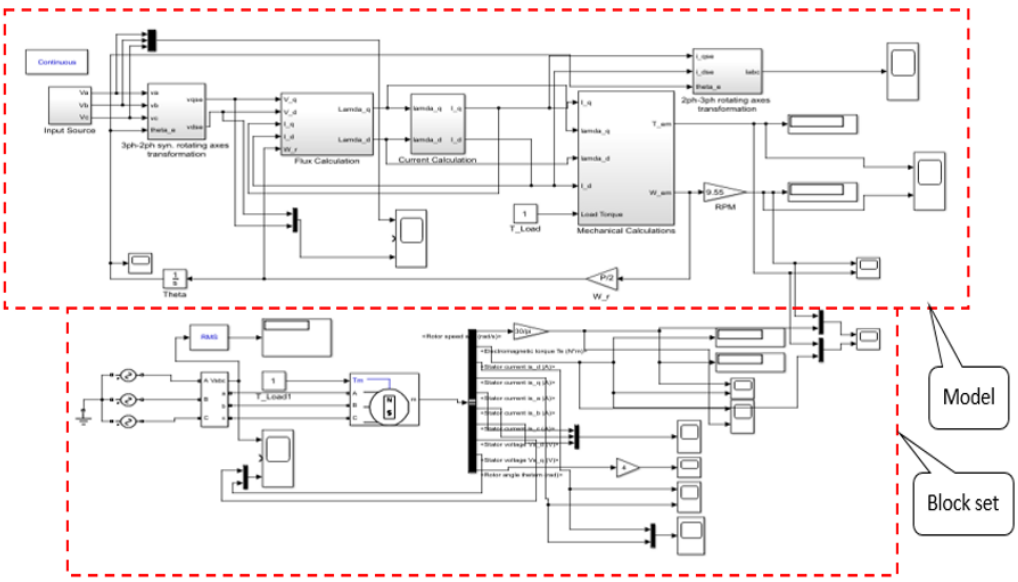

Figure 11. Combined schematisation of the PMSM in the equation model and the Simulink blockset model

variations. The generic mathematical model of the PMSM developed from the fundamental tenet was implemented in MATLAB-Simulink for a specific rating. The suggested simple procedure helps in extracting the required parameters

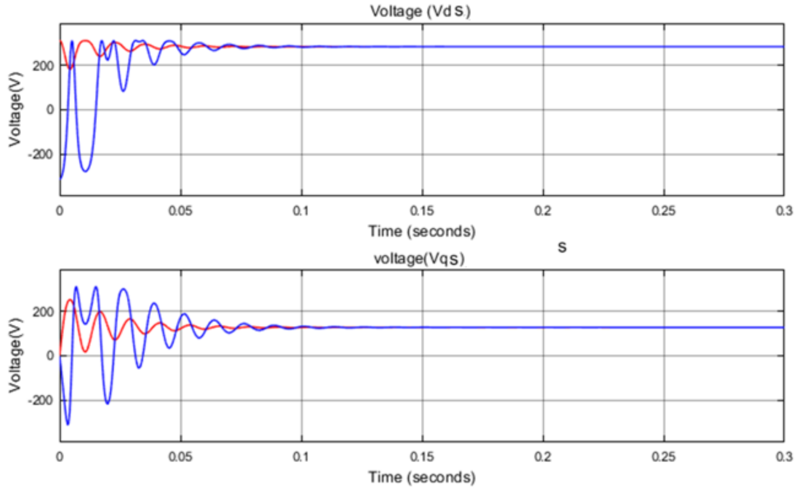

Figure 12. Comparison of responses of the equation and blockset models (d- and q-axis voltage components)

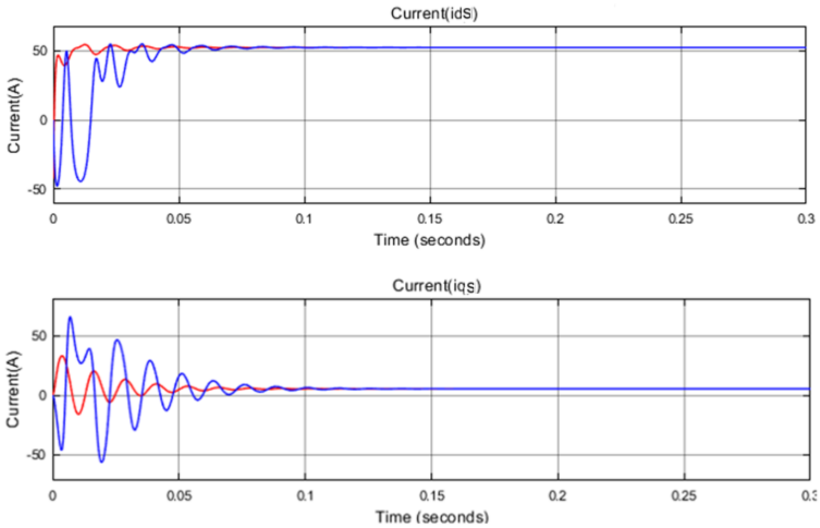

Figure 13. Comparison of responses of the equation and blockset models (d- and q-axis current components)

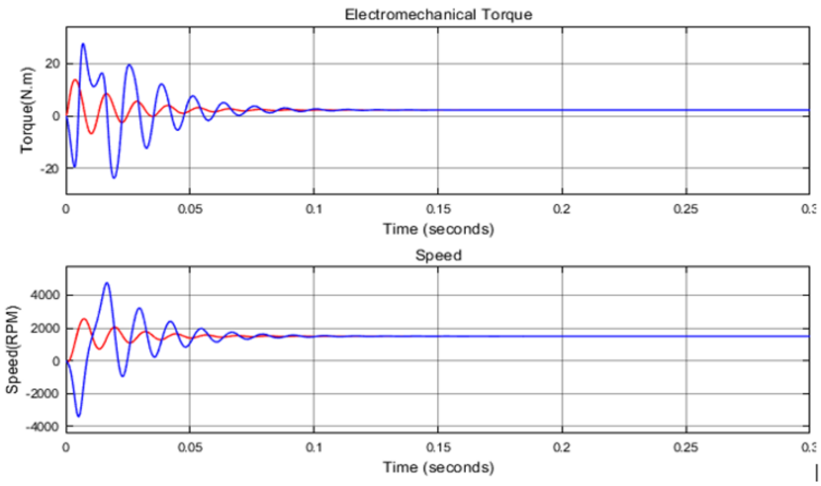

Figure 14. Comparison of responses of the equation and blockset models (torque and speed)

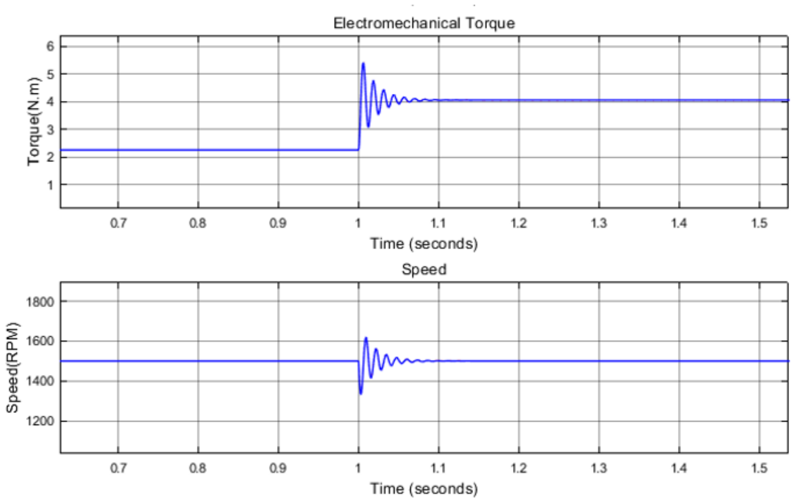

Figure 15. Torque and speed responses for step change load torque (the model in open loop)

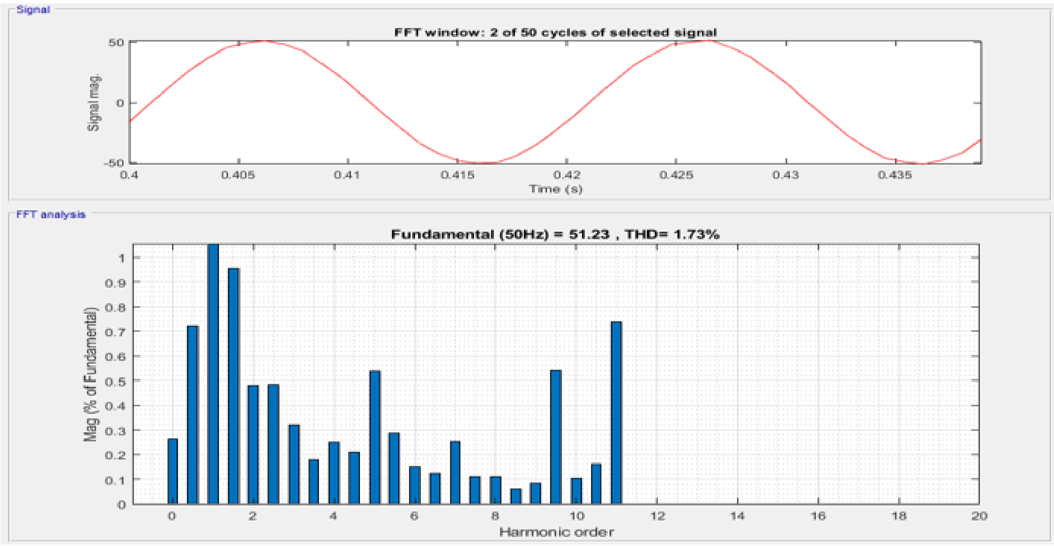

Figure 16. Stator phase current and harmonic spectrum (the equation model)

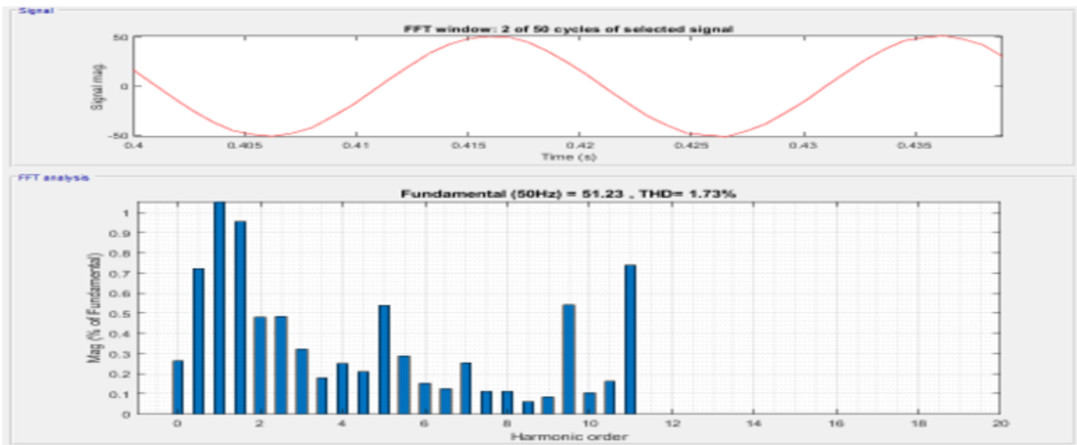

Figure 17. Stator phase current and harmonic spectrum (the blockset model)

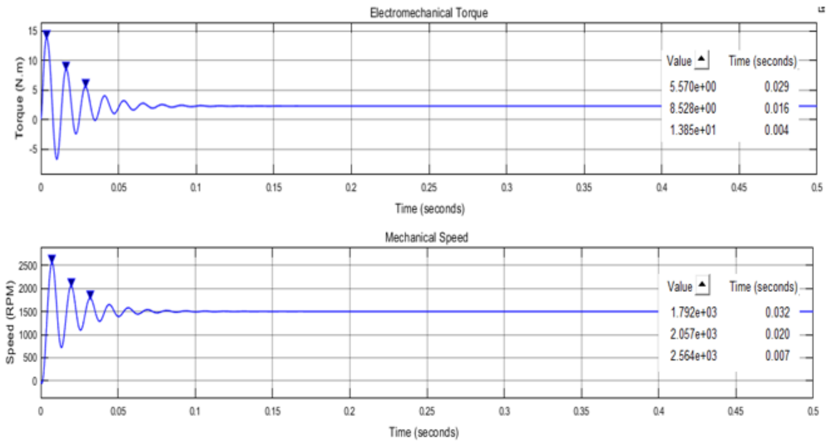

Figure 18. Start up behaviour of torque and speed (the equation model)

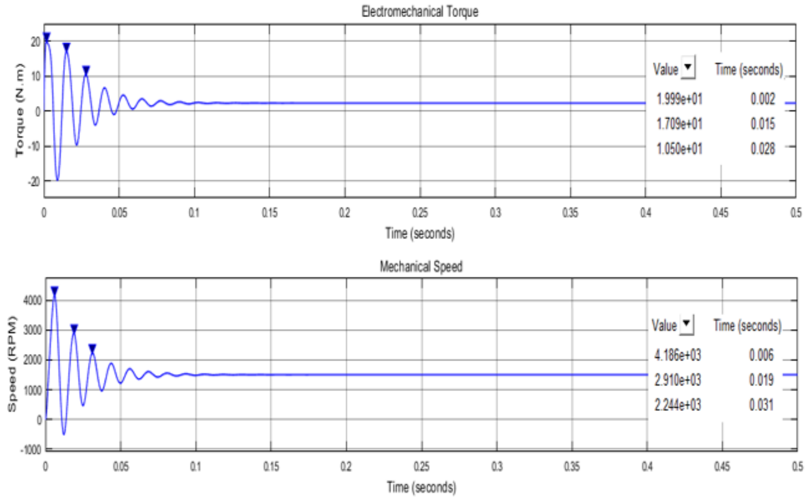

Figure 19. Start up behaviour of torque and speed (the blockset model)

Table 2. Switching states and the corresponding voltages

Metrics	**Model**	**Voltage**		**Current**		**Torque**	**Speed**
		V_{ds}	V_{qs}	I_{ds}	I_{qs}		
Error (%)	Blockset	-	-	-	-	-	-
	Equation	0.41	0.29	0.18	0.18	0.15	0.17
Convergence time (ms)	Blockset	0.107	0.130	0.121	0.132	0.138	0.141
	Equation	0.078	0.092	0.062	0.080	0.071	0.091

for the simulation study from the typical manufacturer's datasheet. The comprehensive comparison between the equation model and the Simulink blockset model for the commercially available PMSMs invigorates the practicing engineers in getting deeper dive on the domain. Research on the PMSM model in open loop at both the studied steady state and transient (step changes) state was conducted. The degree of self-resilience of the motor in open loop against perturbations was validated. The accurateness of the rekindled model was ascertained by comparing it with the MATLAB library blockset. Each model block must be contemplated thoroughly and hence the future customisation will be easy. It should be noted that simultaneously achieving high model accuracy and incorporating multiple criteria may be challenging due to potential contradictions. With the developed accurate model, young researchers can develop closed-loop control focusing on design of both inner and outer loop controllers.

Data Availability

The data used to support the research findings are available from the corresponding author upon request.

Conflicts of Interest

The authors declare no conflict of interest.

References

[1] Z. Guo, J. Zhang, C. Zheng, and Z. Sun, "Dynamic performance analysis of the induction motor drive fed by current-source based on ansoft," *AMSE J. Model. A*, vol. 89, no. 1, pp. 118–129, 2016. http://amse-journals.eu/

[2] V. Yurchenko, V. Pikalov, R. Belokopytov, A. Boykov, and K. Drapak, "Electric drive modernization by replacing brushed DC motor with permanent magnet synchronous motor in rehabilitation robotic system," in *2022 4th International Conference on Control Systems, Mathematical Modeling, Automation and Energy Efficiency (SUMMA)*, Lipetsk, Russian Federation, 2022. https://ieeexplore.ieee.org/document/9999999

[3] F. Oudjama, A. Boumediene, K. Saidi, and D. Boubekeur, "Robust speed control in nonlinear electric vehicles using H-infinity control and the LMI approach," *J. Intell. Syst. Control*, vol. 2, no. 3, pp. 170–182, 2023. https://doi.org/10.56578/jisc020305

[4] D. Schroeder, "Trends in electrical drives for low cost automation," vol. 22, no. 18, pp. 317–327, 1989. https://doi.org/10.1016/S1474-6670(17)52861-X

[5] C. Cronin, A. Awasthi, A. Conway, D. O'Riordan, and J. Walsh, "Design and development of a material handling system for an autonomous intelligent vehicle for flexible manufacturing," *Procedia Manuf.*, vol. 51, pp. 493–500, 2020. https://doi.org/10.1016/j.promfg.2020.10.069

[6] T. W. Ching, "An investigation on electrical performance of variable-frequency drives for air-conditioning applications," in *2008 IEEE Canada Electric Power Conference*, Vancouver, BC, Canada, 2008. https://doi.org/10.1109/EPC.2008.4763323

[7] M. Safaeian, A. Jalilvand, and A. Taheri, "A MRAS based model predictive control for multi-leg based multi-drive system used in hot rolling mill applications," *IEEE Access*, vol. 8, pp. 215 493–215 504, 2020. https://doi.org/10.1109/ACCESS.2020.3041310

[8] D. K. Ray, S. Chattopadhyay, and S. Sengupta, "Multi-resolution analysis based line to ground fault discrimination in standalone wind energy conversion system in harmonic environment," *Lect. Model. Simul. AMSE*, no. 2, pp. 139–150, 2017.

[9] W. Cao, B. C. Mecrow, G. J. Atkinson, J. W. Bennett, and D. J. Atkinson, "Overview of electric motor technologies used for more electric aircraft (MEA)," *IEEE Trans. Ind. Electron.*, vol. 59, no. 9, pp. 3523–3531, 2011. https://doi.org/10.1109/TIE.2011.2165453

[10] N. C. Lenin, "48-volt energy efficient domestic appliances with flux switching motor drive system–design, simulation, and comparison," *IEEE Access*, vol. 10, pp. 81 568–81 580, 2022. https://doi.org/10.1109/ACCESS.2022.3193687

[11] S. S. Rauth and B. Samanta, "Comparative analysis of IM/BLDC/PMSM drives for electric vehicle traction applications using ANN-based FOC," in *2020 IEEE 17th India Council International Conference (INDICON)*, New Delhi, India, 2020. https://doi.org/10.1109/INDICON49873.2020.9342237

[12] K. Algarny, A. S. Abdelrahman, and M. Z. Youssef, "Performance comparison between induction and permanent magnet synchronous electric machines in water pump application," in *2018 2nd European Conference on Electrical Engineering and Computer Science (EECS)*, Bern, Switzerland, 2018. https://doi.org/10.1109/EECS.2018.00038

[13] H. Lee and J. Lee, "Design of iterative sliding mode observer for sensorless PMSM control," *IEEE Trans. Control Syst. Technol.*, vol. 21, no. 4, pp. 1394–1399, 2013. https://doi.org/10.1109/TCST.2012.2199493

[14] J. H. Lee, J. Kim, J. Song, Y. Kim, and S. Jung, "A novel memetic algorithm using modified particle swarm optimization and mesh adaptive direct search for PMSM design," *IEEE Trans. Magn.*, vol. 52, no. 3, pp. 1–4, 2016. https://doi.org/10.1109/TMAG.2015.2482975

[15] S. U. Chung, J. W. Kim, Y. D. Chun, B. C. Woo, and D. K. Hong, "Fractional slot concentrated winding PMSM with consequent pole rotor for a low-speed direct drive: Reduction of rare earth permanent magnet," *IEEE Trans. Energy Convers.*, vol. 30, no. 1, pp. 103–109, 2015. https://doi.org/10.1109/TEC.2014.2352365

[16] C. Olivieri and M. Tursini, "A novel PLL scheme for a sensorless PMSM drive overcoming common speed reversal problems," in *International Symposium on Power Electronics Power Electronics, Electrical Drives, Automation and Motion*, Sorrento, Italy, 2012. https://doi.org/10.1109/SPEEDAM.2012.6264468

[17] R. Yao, "Online d-q axis inductance identification for ipmsms using fea-driven cnn," *Ain Shams Eng. J.*, vol. 15, no. 12, p. 103130, 2024. https://doi.org/10.1016/j.asej.2024.103130

[18] P. Pillay and R. Krishnan, "Modeling of permanent magnet motor drives," *IEEE Trans. Ind. Electron.*, vol. 35, no. 4, pp. 537–541, 1988. https://doi.org/10.1109/41.9176

[19] T. Sebastian, R. Slemon, and M. A. Rahman, “Modelling of permanent magnet synchronous motors,” *IEEE Trans. Magn.*, vol. 22, no. 5, pp. 1069–1071, 1986. https://doi.org/10.1109/TMAG.1986.1064466

[20] C. Bowen, Z. Jihua, and R. Zhang, “Modeling and simulation of permanent magnet synchronous motor drives,” in *ICEMS’2001. Proceedings of the Fifth International Conference on Electrical Machines and Systems (IEEE Cat. No.01EX501)*, Shenyang, China, 2001. https://doi.org/10.1109/ICEMS.2001.971825

[21] H. Zhang, W. Qian, Y. Wu, S. Gan, and Y. Yu, “Modeling and simulation of the permanent-magnet synchronous motor drive,” in *2011 International Conference on Uncertainty Reasoning and Knowledge Engineering*, Bali, Indonesia, 2011. https://doi.org/10.1109/URKE.2011.6007882

[22] G. H. Kang, J. P. Hong, G. T. Kim, and J. W. Park, “Improved parameter modeling of interior permanent magnet synchronous motor based on finite element analysis,” *IEEE Trans. Magn.*, vol. 36, no. 4, pp. 1867–1870, 2000. https://doi.org/10.1109/20.877809

[23] C. Dutta and S. M. Tripathi, “Comparison between conventional and loss dq model of PMSM,” in *2016 International Conference on Emerging Trends in Electrical Electronics & Sustainable Energy Systems (ICETEESES)*, Sultanpur, India, 2016. https://doi.org/10.1109/ICETEESES.2016.7581370

[24] H. Li and X. Jian, “Parameter identification of permanent magnet synchronous motor based on CGCRAO algorithm,” *IEEE Access*, vol. 11, pp. 124 319–124 330, 2023. https://doi.org/10.1109/ACCESS.2023.3330495

[25] M. X. Bui, R. Dutta, and F. Rahman, “Application of deep learning in parameter estimation of permanent magnet synchronous machines,” *IEEE Access*, vol. 12, pp. 40 710–40 721, 2024. https://doi.org/10.1109/ACCESS.2024.3377224

[26] Z. Q. Zhu, D. Liang, and K. Liu, “Online parameter estimation for permanent magnet synchronous machines: An overview,” *IEEE Access*, vol. 9, pp. 59 059–59 084, 2021. https://doi.org/10.1109/ACCESS.2021.3072959